HHS Public Access

Author manuscript

Metabolomics. Author manuscript; available in PMC 2017 August 01.

Published in final edited form as:

Metabolomics. 2016 August ; 12(8): . doi:10.1007/s11306-016-1079-5.

Lung injury-induced skeletal muscle wasting in aged mice is linked to alterations in long chain fatty acid metabolism

D. Clark Files[*],
Internal Medicine-Sections in Pulmonary and Critical Care Medicine and Geriatrics and the Critical Illness Injury and Recovery Research Center, Wake Forest School of Medicine, Winston-Salem, NC USA

Amro Ilaiwy[*],
Sarah W. Stedman Nutrition and Metabolism Center, Duke Molecular Physiology Institute, Duke University Medical Center, Durham, NC, USA; Division of Endocrinology, Metabolism, and Nutrition, Department of Medicine, Duke University Medical Center, Durham, NC, USA

Traci L. Parry,
McAllister Heart Institute, University of North Carolina, Chapel Hill, NC, USA

Kevin W. Gibbs,
Internal Medicine-Section in Pulmonary and Critical Care Medicine

Chun Liu,
Internal Medicine-Section in Pulmonary and Critical Care Medicine

James R. Bain,
Sarah W. Stedman Nutrition and Metabolism Center, Duke Molecular Physiology Institute, Duke University Medical Center, Durham, NC, USA; Division of Endocrinology, Metabolism, and Nutrition, Department of Medicine, Duke University Medical Center, Durham, NC, USA

Osvaldo Delbono,
Internal Medicine-Geriatrics, Wake Forest School of Medicine, Winston-Salem, NC USA

Michael J. Muehlbauer, and
Sarah W. Stedman Nutrition and Metabolism Center, Duke Molecular Physiology Institute, Duke University Medical Center, Durham, NC, USA

Monte S. Willis
McAllister Heart Institute, Department of Pharmacology, Department of Pathology & Laboratory, Medicine, University of North Carolina, Chapel Hill, NC, USA

Abstract

Correspondence to: Monte S. Willis.

[*]D. Clark Files and Amro Ilaiwy have contributed equally.

Conflict of interest: The authors declare that they have no conflict of interest.

Compliance with Ethical Standards: All applicable international, national, and/or institutional guidelines for the care and use of animals were followed.

Introduction—Older patients are more likely to acquire and die from acute respiratory distress syndrome (ARDS) and muscle weakness may be more clinically significant in older persons. Recent data implicate muscle ring finger protein 1 (MuRF1) in lung injury-induced skeletal muscle atrophy in young mice and identify an alternative role for MuRF1 in cardiac metabolism regulation through inhibition of fatty acid oxidation.

Objectives—To develop a model of lung injury-induced muscle wasting in old mice and to evaluate the skeletal muscle metabolomic profile of adult and old acute lung injury (ALI) mice.

Methods—Young (2 month), adult (6 month) and old (20 month) male C57Bl6J mice underwent Sham (intratracheal H_2O) or ALI [intratracheal *E. coli* lipopolysaccharide (i.t. LPS)] conditions and muscle functional testing. Metabolomic analysis on gastrocnemius muscle was performed using gas chromatography-mass spectrometry (GC-MS).

Results—Old ALI mice had increased mortality and failed to recover skeletal muscle function compared to adult ALI mice. Muscle MuRF1 expression was increased in old ALI mice at day 3. Non-targeted muscle metabolomics revealed alterations in amino acid biosynthesis and fatty acid metabolism in old ALI mice. Targeted metabolomics of fatty acid intermediates (acyl-carnitines) and amino acids revealed a reduction in long chain acyl-carnitines in old ALI mice.

Conclusion—This study demonstrates age-associated susceptibility to ALI-induced muscle wasting which parallels a metabolomic profile suggestive of altered muscle fatty acid metabolism. MuRF1 activation may contribute to both atrophy and impaired fatty acid oxidation, which may synergistically impair muscle function in old ALI mice.

Keywords

Aging; muscle atrophy; metabolomics; acute respiratory distress syndrome; intensive care unit acquired weakness; fatty acid metabolism; MuRF1

Introduction

Acute respiratory distress syndrome (ARDS), a syndrome of acute lung inflammation caused by both direct and indirect acute lung insults, affects at least 200,000 persons per year in the United States alone (Force et al. 2012; Rubenfeld et al. 2005). While ARDS mortality has decreased over the past decades (Matthay et al. 2012), a cadre of critical illness survivors has been left in the wake, many of whom are faced with severe functional limitation. One of the serious limitations that intensive care unit survivors face is persistent skeletal muscle weakness, which may persist for years after the resolution of ARDS in many patients (Bienvenu et al. 2012; Herridge et al. 2011). Studies have linked skeletal muscle weakness with mortality. One prospective multicenter cohort study investigated adults requiring at least 5 days of mechanical ventilation without evidence of pre-existing neuromuscular disease. They demonstrated that handgrip strength performed well as a diagnostic for the acquisition of ICU acquired paresis (ICUAP), with handgrip strength independently associated with hospital mortality (OR 4.5, p=0.007) (Ali et al. 2008). In a randomized controlled trial, prospectively collected data has demonstrated the impact of weakness on outcomes and costs in the adult ICU(Hermans et al. 2014). Of 415 long-stay assessable ICU patients, 122 were identified as weak using the MRC sum score (<36, based

on treatment, glucose levels, new infections and time to first MRC reflecting time to awakening) and matched to 122 not-weak patients(Hermans et al. 2014). Weak long-stay ICU patients significantly less likely to wean from mechanical ventilation, leave the ICU, or be discharged from the hospital(Hermans et al. 2014). The in-hospital costs per patients were +30.5% more than the matched not-weak patients and their 1 year mortality was 30.6% (vs. 17.2% in the not-weak group, p=0.007)(Hermans et al. 2014). While these studies demonstrate that ICU-acquired neuromuscular dysfunction independently increases mortality, prolongs duration of mechanical ventilation and contributes to long-term functional impairment (Ali et al. 2008; Hermans et al. 2014), the mechanisms underlying the development ICU acquired neuromuscular dysfunction are incompletely understood and no pharmacologic therapies currently exist.

One well-defined risk factor for both acquisition of and mortality from ARDS is increased age (Amato et al. 2015; Rubenfeld et al. 2005). Older ARDS patients also have profound functional impairment following severe critical illness, suggesting that ICU acquired neuromuscular dysfunction may be more severe in older patients (Ehlenbach et al. 2015; Ely et al. 2002; Ferrante et al. 2015). The etiologies for these potential age-associated disparities in ICU acquired neuromuscular dysfunction in ARDS are unknown, but may relate to the underlying loss of muscle mass and function (sarcopenia) associated with aging (Cruz-Jentoft et al. 2010). Therefore, it is important to understand the fundamental differences in ARDS-induced neuromuscular dysfunction across the age-span, as therapeutic strategies may differ in young and old patients.

Using a previously established model (Files et al. 2012), the present study investigated ALI-induced skeletal muscle wasting in adult (6-month) and old (20-month) lung-injured mice to evaluate potential age-dependent phenotypes. We then examined metabolic differences in the muscles of adult and old mice following lung injury, using both non-targeted and targeted metabolomics approaches. We identified distinct alterations in lipid and amino acid metabolism in the muscles of old ALI mice, paralleling their impaired functional recovery when compared to adult ALI mice.

Materials and Methods

Animals and acute lung injury model

All procedures were approved by the Institutional Animal Care and Use Committee of Wake Forest School of Medicine. 2-month (young), 6-month (adult) and 20-month (old) male wild type C57BL/6 mice (The National Institute of Health Aging Mouse Colony) were anesthetized with an intraperitoneal (i.p.) injection of 150 mg/kg ketamine and 13.5 mg/kg acetylpromazine and the trachea exposed. *Escherichia coli* lipopolysaccharide (LPS) (O55:B5 L2880, lot 111M4035V, Sigma-Aldrich, St. Louis, MO) (ALI mice) at specified, weight-based dosages or an equivalent volume of sterile water (Sham mice) was instilled intratracheally using a 20-gauge catheter as previously described (Files et al. 2012). Mice were observed for up to 10 days and harvested at specified time points. Daily food intake per mouse was obtained by weighing the daily food mass per cage divided by the number of mice in the cage in adult and old mice at baseline and following ALI conditions.

In vivo force measurements

Force measurements were made with an *in-vivo* force transducer (Aurora Scientific, Aurora, Ontario, Canada) that measures force generation *in-vivo* longitudinally over time in a single animal. Briefly, this apparatus measures force production by plantarflexion of the ankle mounted to a foot-plate to which the mouse hind foot is attached. Animals were anesthetized with 2% inhaled isoflurane at a constant flow rate of 2 liters/minute. After removal of the animal's fur, the tibial nerve was located and an electrode was placed over the nerve. Resting tension, muscle length and stimulation current were iteratively adjusted for each muscle to obtain optimal twitch force. The nerve was then stimulated with 250 millisecond trains of pulses at increasing frequencies every 2 minutes and the maximum tetanic force was recorded for the force-frequency curves. The maximal force generated for each contraction was plotted as a percentage of the initial maximal force over the duration of the fatigue protocol. For the studies described, baseline force measurements were obtained on uninjured adult and old mice. Following the lung injury protocol at 0.75 μg/g or 1 μg/g LPS (low dose LPS), measurements were obtained again on days 3 and 10. The data is displayed as the percent change from baseline force at days 3 or 10 from the maximal tetanic forces generated at 125 Hz at each of these time points and is combined from two independent experiments.

Muscle extraction and morphometry

Following euthanasia, gastrocnemius (GAS), extensor digitorum longus (EDL), soleus (SOL) and tibialis anterior (TA) muscles were removed, blotted with tissue paper and immediately weighed. Muscles were snap frozen in liquid nitrogen as previously described (Files et al. 2015a). Soleus muscles were prepared as previously described for muscle morphometry. For fiber typing data, type I or type II myofibers of the soleus muscle were identified using the ATPase method at pH 9.4 as previously described (Files et al. 2012). Soleus muscle lipid content was identified on serial sections, using the Oil Red O (Poly Scientific R&D) staining method. Lipid droplet size measurements were obtained in at least 20 myofibers per muscle section and quantified using Image J® software (NIH, Bethesda MD) as previously described (Choi et al. 2016).

Western blotting

Western blotting was performed as previously described using the following antibodies: Trim63 (MuRF1) (AF5366 R&D Systems, Minneapolis, MN, USA), GAPDH (AM4300 Ambion, Austin, TX, USA) (Files et al. 2015a).

Non-targeted metabolomics determination by GC–MS instrumentation

Gastrocnemius muscle tissue was flash frozen in a liquid nitrogen, weighed (25–50 mg wet weight), then placed in buffer (50 % acetyl-nitrile, 50 % water, 0.3 % formic acid) at a standard concentration of 25 mg/475 μl buffer then fully homogenized on ice for 10–25 s and placed on dry ice/stored at -80C. Samples were then analyzed by GC/MS, as previously described (Banerjee et al. 2015). The raw, transformed, and sorted data used for each of the three comparisons in the metabolomics analyses can be found in Supplemental Table 1. In the acute lung injury studies, four groups of ten samples were analyzed (40 total). If more

than 3 individuals did not have a metabolite detected in a group (of 10 total), they were excluded from further analysis for that metabolite. In groups with fewer values missing, the lowest value of that group was used to impute those values. Supplemental Table 1 contains raw and imputed data sets including targeted and non-targed data and has been submitted to the UCSD metabolomics Workbench (http://www.metabolomicsworkbench.org/), accession number pending (uploaded March 21 2016). The MuRF1 Tg+ and MuRF1-/- metabolomics data was similarly analyzed, which included four groups (MuRF1 Tg+, strain-matched wildtypeMuRF1Tg+, MuRF1-/-, and strain-matched MuRF1+/+) with three replicates. Missing values were imputed only if 1 was missing; groups with 2 or more missing values were excluded from analysis for that metabolite. Supplemental Table 2 contains raw and imputed data sets including both targeted and non-targeted data.

Targeted metabolomics of acyl-carnitine and amino acid quantification by GC–MS instrumentation

Amino acids and acyl-carnitines were analyzed using stable isotope dilution techniques. Amino acids and acyl-carnitine measurements were made by flow injection tandem mass spectrometry using sample preparation methods described previously(An et al. 2004; Jensen et al. 2006; Wu et al. 2004). The data were acquired using a Waters Acquity™ UPLC system equipped with a TQ (triple quadrupole) detector and a data system controlled by MassLynx 4.1 operating system (Waters, Milford, MA). Metabolite concentrations were analyzed using Metaboanalyst v3.0 (Xia et al. 2009; Xia et al. 2015; Xia et al. 2011) run in the statistical package R (v2.14.0). Initial unsupervised evaluation using principal component analysis (PCA) identified the presence of acute lung injury as the primary source of variance. Data were next analyzed using PLSDA and VIP analyses in a similar manner to what was previously described. Metabolites that best differentiated the groups were individually tested using Metaboanalyst v3.0 t-test feature. Of note, metabolites were normalized by reference sample created from Sham group average.

Metabolomic Statistical Analyses

Metaboanalyst (v3.0) run on the statistical package R (v2.14.0) used metabolite peaks areas (as representative of concentration)(Xia et al. 2009; Xia et al. 2015). These data were first normalized to a pooled average sample created from their control- Sham group, and scaled using Pareto scaling feature, and then analyzed to calculate Fold change using Metaboanalyst fold change feature. Unsupervised principal component analysis (PCA) was performed next, which identified the presence of the acute lung injury in the mice as the principal source of variance. The metabolites that best differentiated the groups were then individually tested using univariate analysis of individual component by t-test (Metaboanalyst v3.0), and then both the t-test and VIP significant metabolites were matched to metabolomics pathways using the Pathway Analysis and enrichment analysis features in Metaboanalyst v3.0. To detect systemic metabolic signature of ALI in the context of age, a One-Way Analysis of Variance (ANOVA) and Fisher LSD post-hoc test across the two ages (adult, old) and experimental groups (sham, ALI)(adult sham, adult ALI, old sham, old ALI) using Metaboanalyst v3.0 including p values. Similarly, the metabolic signatures from these gastrocnemius groups were compared to MuRF1 Tg+ and MuRF1-/- hearts using a One-Way Analysis of Variance (ANOVA) and Fisher LSD post-hoc test to compare adult Sham,

adult ALI, old Sham, old ALI, wildtype$^{MuRF1Tg+}$, MuRF1 Tg+, MuRF1+/+, MuRF1-/-. Only metabolites identified and detected in all groups were included in the One-Way ANOVA. If four or more values of each metabolite were missing in a given group, the entire metabolite was removed from the analysis. Only metabolites significantly altered in 2 or more organs were plotted. Data used in this study are available in Supplemental Table 1 and Supplemental Table 2. Heat maps were generated using the GENE- E software (http://www.broadinstitute.org/cancer/software/GENE-E/index.html).

Other Statistical Analyses

All data is shown as mean +/- SEM, unless otherwise indicated. Differences between two groups were compared with the Student's t test or the Mann-Whitney test for nonparametric data, while comparisons between >2 groups used a One-Way ANOVA. Post-hoc analysis was performed using a t-test with the Bonferroni adjustment method using Prism 7.0 (GraphPad Software, Inc., La Jolla, CA).

Results

Instillation of lipopolysaccharide (LPS) at a dose previously established to cause a survivable lung injury and muscle wasting in young mice caused a step-wise and age-dependent increase in mortality. At 10 days following intratracheal (i.t) LPS, 87% of young and 77% of adult mice survived, but none of the old mice did (Figure 1A). Since this paradigm did not allow investigation of chronic skeletal muscle alterations post-acute illness, we adjusted the model to create a reproducible survival model of ALI in old mice. To do this, we incrementally reduced the LPS dose and observed the dose-related survival response. We found that reducing the dose to 0.75 or 1 μg/g LPS (low dose LPS) led to survival in ~75% of the old ALI mice and 100% survival in adult ALI mice (Figure 1B). Low dose i.t. LPS caused profound body weight loss (Figure 1C) in both adult and old ALI mice during the early phase (days 0 through 5), though maximal body weight loss peaked at day 3 in adult ALI mice (16% below baseline) and body weight loss peaked at day 5 in old ALI mice (21% below baseline). During the late phase (days 6 through 10), both adult and old ALI mice gained weight at a similar rate, but the old ALI mice body weight recovery started from a lower baseline. Mean daily baseline food intake was similar in young (3.7 g/day) and old (3.2 g/day) mice. Following low dose ALI, food intake dropped to ~12% of baseline daily food intake for the first 2 days in both groups, and then slowly increased through day 9 where they were similar to the baseline levels of daily food intake (Figure 1D).

Despite body weight recovery in old ALI mice during the late phase, muscle function failed to recover. Maximal tetanic force generated from the hindlimb ankle plantar flexor muscle group in the adult and old mice at baseline, days 3 and 10, was reduced in old ALI mice at day 10 (compared to both old baseline and adult ALI mice at day 10). In contrast, there was no evidence of significant weakness from baseline levels in adult ALI mice at either timepoint (Figure 1E). Analysis of the tibialis anterior (TA) and extensor digitorum longus (EDL) wet weights demonstrated reduced muscle mass both adult and old ALI mice at day 10, although the percent of muscle mass lost in old ALI mice (vs old Sham) was equivalent

or less than that observed in the adult ALI mice (vs adult Sham) (Figure 1F, G). In contrast, muscle mass was preserved in the soleus in both adult and old ALI mice (Figure 1H), supporting a relative preservation of type I myofibers in the limb muscles under ALI conditions (Files et al. 2015a).

Previous studies have implicated the muscle specific ubiquitin ligase (MuRF1) in skeletal muscle atrophy (Bodine et al. 2001), and have demonstrated that MuRF1 expression is necessary to cause ALI-induced muscle atrophy (Files et al. 2012; Langen et al. 2012). We then investigated MuRF1 protein in all groups. Western blot analysis of MuRF1 in the gastrocnemius muscle, a mixed fiber type muscle, identified significant upregulation in both adult and old ALI mice (compared to Sham), which was higher in the old ALI mice compared to adult ALI mice at day 3 (Figure 1I). However, at day 10, when old ALI mice displayed profound muscle weakness, MuRF1 levels had returned to baseline (Figure 1J). This finding, along with the lack of reduced muscle mass at day 10, suggest that atrophy does not account for the loss of muscle function in old mice at day 10. Further histological evaluation of soleus muscle in ALI mice revealed increased intramyocellular lipid (IMCL) droplet size in old versus young ALI mice at day 10 in both type I and type II myofibers (Figure 1K), a finding associated with both impaired skeletal muscle function (Choi et al. 2016; Picard et al. 2012) and metabolism (Consitt et al. 2009) in previous studies.

To explore potential underlying muscle metabolic defects in adult and old ALI mice during the late phase, we performed non-targeted metabolomics analysis on gastrocnemius muscle samples of adult and old, Sham and ALI mice at day 10. We first compared the adult ALI to adult Sham groups (Figure 2), then similarly analyzed the old ALI muscle metabolomic profile (Figure 3). Analysis of the adult ALI gastrocnemius profile identified 111 metabolites, 66 of which were named (Figure 2A). A supervised partial least squares regression discriminant analysis (PLS-DA) identified distinct alterations in the metabolomics profile, with the first principal component accounting for 28.6% of the differences observed between groups (Figure 2B). The associated Variable Importance in Projection (VIP) analysis identified 5 metabolites with VIP scores >2, including lactic acid, taurine, cholesterol, glucose-6-phosphate, and glucose and other aldohexoses (Figure 2C). A t-test analysis identified 9 metabolites to be significantly different, including hydroxyprolines, glutamine, beta-alanine, aminomalonic acid, and linoleic acid that were significantly decreased 20-30% or significantly increased 30-236% from controls (Figure 2D)($p<0.05$). Parallel analysis of the old ALI muscle compared to old Sham identified 111 metabolites, 69 of which were named (Figure 3A). PLS-DA identified distinct alterations in the metabolomic profile, with the first principal component accounting for 35.6% of the differences observed between groups (Figure 3B). The associated Variable Importance in Projection (VIP) analysis identified 3 metabolites with VIP scores >2, including lactic acid, phosphoric acid, and glucose/other aldohexoses (Figure 3C). A t-test analysis identified 18 metabolites, including elevations in 2-aminoadipic acid, hydroxyprolines, lysine, linoleic acid, glutamic acid, aspartic acid, and phenylalanine to be significantly decreased to 55-85% or significantly increased 33-233%) compared to old Sham muscle (Figure 3D)($p<0.05$). In contrast to the adult ALI gastrocnemius, the old ALI gastrocnemius generally had more significantly different amino acids (5 in old ALI compared to 3 in the adult ALI), and fatty acids identified by t-test (5 in old ALI compared to 2 in the adult ALI).

We next sought to determine what underlying pathways were altered in the adult and old ALI muscle using the specific metabolites identified in Figure 2D and Figure 3D as t-test and VIP significant. Using pathway enrichment analysis, we identified metabolomics alterations in the adult ALI enriched primarily in Inositol phosphate, pyrimidine, galactose and D- glutamine metabolism (Figure 4A), reflected in Ammonia Recycling pathway enrichment of 6+ fold and the lowest p value (Figure 4B). Additional enrichment analyses against disease-associated metabolite sets identified mammary-tumor-bearing mice and 3-methylglutaonic aciduria (type II) (Supplemental Figure 1A), Alzheimer's disease, and 2-methyl-3-hydroxybutyryl-CoA dehydrogenase deficiency (Supplemental Figure 1B) with the lowest p values. Enrichment based on location identified the basal ganglia (Supplemental Figure 1C) with the lowest p value. Pathway enrichment analysis in the old ALI muscle revealed alterations in lysine biosynthesis, amino acids biosynthesis and biosynthesis of unsaturated fatty acids ($p<0.05$) (Figure 4C). Further enrichment analysis of pathway-associated metabolite sets highlighted significant enrichment of alpha-linoleic acid and linolenic acid metabolism (>9 fold enrichment), glucose-alanine cycle (7 fold enrichment), biotin metabolism (10 fold enrichment) and protein biosynthesis (7 fold enrichment and lowest p value) (Figure 4D). Additional enrichment analyses against disease-associated processes identified alterations with the lowest p value associated with the 2-ketoglutarate dehydrongenase process (Supplemental Figure 2A), Glut-1 deficiency (Supplemental Figure 2B), 2-methyl-3-hydroxybutyryl-CoA dehydrogenase deficiency and metabolic enrichment in bladder and skeletal muscle (Supplemental Figure 2C). Interestingly, both adult and old ALI muscle was enriched for 2-methyl-3-hydroxybutyryl-CoA dehydrogenase deficiency, an inborn error caused by a defect in the degradation of the branched chain amino acid isoleucine. Characterized by severe motor defects, disrupted mitochondria, and accumulation of intracellular lipids, 2-methyl-3-hydroxybutyryl-CoA dehydrogenase deficiency exhibit aspects of altered fatty acid metabolism (Chatfield et al. 2015). Together, these findings helped focus our attention on the amino acid and fatty acid metabolic alterations in ALI muscle for further targeted analysis.

Next, we next performed a targeted quantitative analysis of 15 amino acids and 40 acyl-carnitines (grouped into short, medium, and long chain acyl-carnitines) on adult ALI (Figure 5A) and old ALI muscle (Figure 5D). The Unsupervised PCA analysis of targeted metabolomics between adult ALI and adult Sham mice groups revealed that alanine as the only metabolite with a VIP score >2 (Figure 5B). Three t-test significant metabolites were also identified: 1) histidine, 2) citrulline, and 3) ornithine (Figure 5C). Complementary studies of the old ALI muscle (Figure 5D) revealed that alanine and glutamine had VIP scores >2 (Figure 5E). Similar to the adult ALI, the old ALI had t-test significant increases in citrulline and ornithine (Figure 5F), but uniquely old but not adult ALI mice had a nearly 50% reduction in long chain acyl-carnitines (Figure 5F).

To delineate the underlying mechanisms occurring in both an age-dependent and ALI-dependent manner across all four groups studied, we next performed a One-Way ANOVA across both adult and old Sham and ALI groups (Figure 6). Of the 64 metabolites identified in all four groups (Figure 6A), unique PCA patterns were seen between the four groups (Figure 6B). 22 metabolites were significantly different using ANOVA analysis (Figure 6C). Further inter-group analysis identified age-dependent differences, between old Sham and

adult Sham muscle in metabolites including docosahexaenoic acid, 2-aminoadipic acid, pyruvic acid, lysine, and ononitol (see $, Figure 6C). In addition to these metabolites that were different between the adult Sham and old Sham muscle, we also evaluated metabolite alterations in both old groups (old Sham and old ALI) and identified urea and docosahexanoic acid (DHA)(Supplemental Figure 3A). To identify metabolites that were significantly altered in ALI regardless of age, we identified altered metabolites found in both ALI groups (Supplemental Figure 3A). DHA was significantly increased in an age-dependent fashion (Supplemental Figure 3B), whereas linoleic acid was significantly increased in with ALI conditions regardless of age (Supplemental Figure 3C). In addition, lactate, serine, and alanine were differentially regulated in ALI conditions regardless of age (Supplemental Figure 3A).

In order to further examine potential changes in of acyl-carnitines observed in old ALI mice, we grouped measured acyl-carnitines by chain length and plotted the fold change in old ALI versus old Sham muscle against carbon chain length. This analysis further illustrates that the long chain species were most affected (Supplemental Figure 4). These alterations were reminiscent of the reduced long chain acyl-carnitines seen with increased MuRF1 expression in a prior metabolomics cardiac muscle analysis (Rodriguez et al. 2015). To determine if there were any similarities in the present study (particularly old ALI) with altered MuRF1 signatures in the heart, we performed an ANOVA across the four groups in the present study with the four groups in our previous study (MuRF1 Tg+ and MuRF1-/- and their strain matched controls). Significant alterations in both the grouped long chain (C14-C22) and short chain (C2-C5) acyl-carnitines were seen, along with specific species (Supplemental Figure 5A). Interestingly, the total long chain acyl-carnitines (C14-C22) were significantly depressed similarly to the MuRF1 Tg+ hearts, with the MuRF1-/- hearts having significantly increased levels of total long chain acyl carnitines (Supplemental Figure 5B). We then plotted all of the acyl-carnitines C2-C20 levels for each of the four groups compared to their wildtype controls, which run along the dotted line at 1.0 (Supplemental Figure 5C). We find that the old ALI and MuRF1 Tg+ hearts with increased cardiomyocyte MuRF1 expression follow a parallel acyl-carnitine reduction, affecting the longer acyl-carnitines most (Supplemental Figure 5C, red and green lines). Similarly, adult ALI muscle has reduced levels of longer chain acyl-carnitines (blue line), but are not as severely affected as the old ALI mice. In contrast, the loss of MuRF1 (MuRF1-/- hearts) have increased levels of short and medium chain acyl-carnitines, with the largest increases (compared to wildtype) being in the long chain acyl-carnitine species (gray line)(Supplemental Figure 5C). The significantly altered acyl-carnitine species (vs. adult Sham) determined by ANOVA in any group are indicated in Supplemental Figure 5D, having enrichment for cyanoaminoacid, linoleic, and methane metabolism (Supplemental Figure 6).

Discussion

The relationship between age and increased incidence of and mortality from acute lung injury (ALI)/acute respiratory distress syndrome (ARDS) has been established in both humans and animal models (Manzano et al. 2005; Prows et al. 2015; Rubenfeld et al. 2005). Increasing evidence suggests that neuromuscular weakness developing from critical illness is independently associated with morbidity and mortality, and is therefore an attractive

therapeutic target (Ali et al. 2008; Hermans et al. 2014). While it has been suggested that older patients exhibit increased the severity of ICU acquired neuromuscular weakness, this has been understudied and the mechanisms are unknown (Ehlenbach et al. 2015; Ely et al. 2002; Ferrante et al. 2015; Ferrante et al. 2016). In this manuscript, we present a model of an age-associated increase in mortality from lung injury, coupled with prolonged neuromuscular dysfunction. Muscle wasting in old ALI mice is associated with increased MuRF1 expression during the early phase relative to adult mice; however, no difference is observed in MuRF1 expression in the late phase. Additionally, similar or decreased relative muscle loss is observed in the old mice in the late phase, suggesting that prolonged muscle weakness is due to processes other than muscle atrophy.

The dissociation of muscle mass and muscle strength found in the present study has been previously described in various conditions, including sarcopenia (Baehr et al. 2016; Goodpaster et al. 2006; Metter et al. 1999). The potential physiologic explanations for this dissociation are many, including neuropathies, neuromuscular junction injury, and excitation-contraction uncoupling among others. In light of our findings of profound metabolic alterations during the late phase of lung injury, we believe changes in muscle metabolism represent a potential mechanism underlying the dissociation between muscle mass and function. Previous work has demonstrated that changes in energy substrate and utilization (metabolism) can affect muscle performance (Li et al. 2015; Pugh et al. 2013). While the mechanistic link between the metabolic changes seen in old mouse muscle and the reduction in muscle contractile force are not fully elucidated in this study, we find increased size of intramyocellular lipid droplets in old ALI muscle at day 10. Other studies have found an association between intramyocellular lipid accumulation and impaired muscle contractility in mice and humans (Choi et al. 2016; Duval et al. 2007; Picard et al. 2012; Pugh et al. 2013), though the mechanisms underlying this association remain unclear.

Age-related changes have been identified in rat muscle related to glycolytic metabolism (32 month vs. 15 month rats) (Garvey et al. 2014). Specifically, an accumulation of glycolytic, glycogenolytic, and pentose phosphate pathway intermediates in addition to increases in monounsaturated fatty acids (e.g. oleate and palmitoleate) were found in aged rat gastrocnemius (Garvey et al. 2014). The age-associated increases in long chain fatty acids (oleate and palmitoleate) found in this study, are similar to our findings of elevated long chain polyunsaturated docosahexaenoic acid (DHA) in old versus adult Sham mice. Low plasma DHA levels in cancer patients have been associated with myosteatosis, and supplementation with DHA and other ω-3 fatty acids may improve muscle function in this population (as recently reviewed (Ewaschuk et al. 2014)). The etiology and causality of elevated DHA in the muscle of old mice from our study is unclear. This finding may reflect an inability of old muscle to utilize DHA, or alternately, DHA may be a compensatory adaptive response in aged muscle. As dietary supplementation with DHA holds potential for therapy for muscle wasting in cancer and other conditions, further study is needed to explain the etiology of DHA and other long chain fatty acids in aged muscle (Ewaschuk et al. 2014; Kamolrat, Gray 2013; Smith et al. 1999).

The poly-unsaturated ω-6 fatty acid, linoleic acid was significantly increased after ALI in both adult and old mice. While a mechanistic link between ALI and increased linoleic acid

in muscle is not clear, several studies have linked alterations in plasma linoleic acid with acute lung injuries, including ARDS, pneumonia, and septicemia though underlying mechanisms appear unclear (Kumar et al. 2000; Prabha et al. 1991). While these alterations have been implicated in ARDS pathogenesis, their roles still remain unclear. The potential role of enhanced inflammation and utilization of polyunsaturated fatty acids via lipid peroxidation (Quinlan et al. 1996) deserves further study.

Linoleic acid is a substrate required for inflammation, but has also been proposed as an antiinflammatory therapy for skeletal muscle disorders (Tarnopolsky, Safdar 2008; Tian et al. 2011). Conjugated linoleic acid has been used therapeutically and for its anti-inflammatory properties (Larsen, Crowe 2009; Pariza et al. 1999; Zulet et al. 2005), however, its use to protect against muscle weakness has not specifically been investigated. While linoleic acid unexpectedly was not protective in a tumor-mediated model of skeletal muscle atrophy using the C26 cell line in vivo, it enhanced markers of inflammation (Tian et al. 2011). In resistance training, the addition of conjugated linoleic acid has been shown to reduce body fat after 6-months of resistance training in older adults (Tarnopolsky, Safdar 2008). The observed increase in muscle linoleic acid in our study may reflect its role as a substrate for inflammation used to mobilize energy stores from fat systemically. Further work is needed to evaluate the etiology of this pathway in skeletal muscle functional recovery in the ALI model.

The significant decrease in long chain acyl-carnitines that were unique to the old ALI muscle suggests impaired uptake and/or utilization of long chain fatty acids for β oxidation. We also found that old ALI muscle closely parallels a similar acyl-carnitine profile from the MuRF1 Tg+ hearts and contrasts the observed profile in MuRF1-/- hearts. Since MuRF1 is elevated to a greater degree in old compared to adult ALI mice during the early phase, these alterations in acyl-carnitine levels may reflect increased MuRF1 activity in old ALI mice. The mechanism in the heart for this inhibition of fatty acid oxidation has been found to be due to MuRF1 mono-ubiquitination of PPARα, which targets PPARα for nuclear export thereby decreasing PPARα activity (Rodriguez et al. 2015). Further studies are needed to evaluate the potential link between elevated MuRF1 and the observed metabolomic pattern of impaired fatty acid oxidation in the muscles of old ALI mice.

Subsets of patients with a variety of diseases affecting seemingly disparate organ systems experience muscle wasting syndromes, which are associated with poor outcomes (Morley et al. 2006). However, the kinetic relationship between muscle wasting and the presence of the underlying disease in various muscle wasting syndromes appear to differ. For instance, in diseases such as cancer, heart failure and chronic obstructive pulmonary disease (COPD), muscle wasting occurs in parallel with the ongoing disease state. In contrast, in critical illnesses, such as ARDS or sepsis, a massive inflammatory response likely drives the initial muscle injury, yet weakness persists in many patients despite resolution of the initial disease process (Files et al. 2015b). While the muscle proteolytic response in these diseases many have common underlying mechanisms, such as MuRF1 involvement (Bodine, Baehr 2014), the differing kinetics suggest that the underlying mechanisms and metabolic responses might differ.

Recent studies have demonstrated that the metabolomics profiles of muscle atrophy are different depending upon the underlying causes of muscle loss. In healthy mice challenged with cancer (no cachexia/muscle loss), cancer cachexia (early and late time points), calorie restriction-induced muscle loss, and a control group, NMR analysis of serum identified distinct profiles of the cancer cachexia compared to other groups (hyperlipidemia, hyperglycemia, reduced branched-chain amino acids) (Der-Torossian et al. 2013). While these findings confirmed previous studies finding increases in cancer-cachexia plasma (O'Connell et al. 2008), they offered a proof that cure (by surgical resection) paralleled predictable resolution of these changes (Der-Torossian et al. 2013). In another model of cancer cachexia, incubation of human muscle cells with cachectic conditioned media led to upregulation of fatty acid metabolism pathways and in increase in acyl-carnitines. This process was associated with muscle atrophy, and inhibition of FA metabolism attenuated atrophy (Fukawa et al. 2016). These studies demonstrate similarities to our present work, but differences may be due to the methodologies employed (NMR), the differences in the metabolite kinetics between disease processes, age differences, and the lack of ongoing atrophy in the clinically relevant present model. Future studies should evaluate the plasma and muscle metabolomics response during the early phase of our model and investigate the mechanistic link to MuRF1 to determine its potential as a therapeutic target. These studies might shed light on common metabolic mechanisms that may underlie muscle wasting in various disease states.

Conclusions

- Acute lung injury (ALI) in old mice reproduces the observed increase in mortality and muscle weakness in older humans with ALI/ARDS.
- The early phase of muscle wasting in old ALI mice is marked by increased MuRF1, while the late phase is marked by prolonged neuromuscular weakness and metabolomics alterations despite cessation of atrophy.
- Age-dependent muscle metabolite alterations included altered DHA and urea concentrations. ALI-dependent muscle metabolite alterations included linoleic acid, lactate, serine, and alanine, with old ALI muscle demonstrating significantly higher levels of linoleic acid than adult ALI.
- Long chain (C14-C22) acyl-carnitine species were depressed in old ALI muscle suggestive of impaired uptake or utilization of long chain fatty acids for β oxidation.
- The acyl-carnitine profile in old ALI muscle in the late phase coupled with early MuRF 1 upregulation during the early phase parallels the MuRF1 Tg+ cardiac muscle profile, suggesting that MuRF1 may contribute to the metabolic changes in old ALI muscle.

Supplementary Material

Refer to Web version on PubMed Central for supplementary material.

Acknowledgments

This work was supported by the National Institutes of Health (R01HL104129 to M.W.), the Leducq Foundation Transatlantic Networks of Excellence (to M.W.), the Claude D. Pepper Older Americans Independence Center (P30AG21332 to D.C.F and O.D.), and the American Thoracic Society Foundation (D.C.F.).

References

Ali NA, et al. Acquired weakness, handgrip strength, and mortality in critically ill patients. Am J Respir Crit Care Med. 2008; 178:261–8. DOI: 10.1164/rccm.200712-1829OC [PubMed: 18511703]

Amato MB, et al. Driving pressure and survival in the acute respiratory distress syndrome. N Engl J Med. 2015; 372:747–55. DOI: 10.1056/NEJMsa1410639 [PubMed: 25693014]

An J, et al. Hepatic expression of malonyl-CoA decarboxylase reverses muscle, liver and whole-animal insulin resistance. Nat Med. 2004; 10:268–74. DOI: 10.1038/nm995 [PubMed: 14770177]

Baehr LM, et al. Age-related deficits in skeletal muscle recovery following disuse are associated with neuromuscular junction instability and ER stress, not impaired protein synthesis. Aging (Albany NY). 2016; 8:127–46. [PubMed: 26826670]

Banerjee R, et al. Non-targeted metabolomics of double-mutant cardiomyocytes reveals a novel role for SWI/SNF complexes in metabolic homeostasis. Metabolomics. 2015; 11:1287–1301. DOI: 10.1007/s11306-015-0786-7 [PubMed: 26392817]

Bienvenu OJ, et al. Depressive symptoms and impaired physical function after acute lung injury: a 2-year longitudinal study. Am J Respir Crit Care Med. 2012; 185:517–24. DOI: 10.1164/rccm.201103-0503OC [PubMed: 22161158]

Bodine SC, Baehr LM. Skeletal muscle atrophy and the E3 ubiquitin ligases MuRF1 and MAFbx/atrogin-1. Am J Physiol Endocrinol Metab. 2014; 307:E469–84. DOI: 10.1152/ajpendo.00204.2014 [PubMed: 25096180]

Bodine SC, et al. Identification of ubiquitin ligases required for skeletal muscle atrophy. Science. 2001; 294:1704–8. DOI: 10.1126/science.1065874 [PubMed: 11679633]

Chatfield KC, et al. Mitochondrial energy failure in HSD10 disease is due to defective mtDNA transcript processing. Mitochondrion. 2015; 21:1–10. DOI: 10.1016/j.mito.2014.12.005 [PubMed: 25575635]

Choi SJ, et al. Intramyocellular Lipid and Impaired Myofiber Contraction in Normal Weight and Obese Older Adults. J Gerontol A Biol Sci Med Sci. 2016; 71:557–64. DOI: 10.1093/gerona/glv169 [PubMed: 26405061]

Consitt LA, Bell JA, Houmard JA. Intramuscular lipid metabolism, insulin action, and obesity. IUBMB Life. 2009; 61doi: 10.1002/iub.142

Cruz-Jentoft AJ, et al. Sarcopenia: European consensus on definition and diagnosis: Report of the European Working Group on Sarcopenia in Older People. Age Ageing. 2010; 39:412–23. DOI: 10.1093/ageing/afq034 [PubMed: 20392703]

Der-Torossian H, et al. Cancer cachexia's metabolic signature in a murine model confirms a distinct entity. Metabolomics 7, Metabolomics. 2013; doi: 10.1007/s11306-012-0485-6

Duval C, Camara Y, Hondares E, Sibille B, Villarroya F. Overexpression of mitochondrial uncoupling protein-3 does not decrease production of the reactive oxygen species, elevated by palmitate in skeletal muscle cells. FEBS Lett. 2007; 581:955–61. DOI: 10.1016/j.febslet.2007.01.085 [PubMed: 17303124]

Ehlenbach WJ, Larson EB, Randall Curtis J, Hough CL. Physical Function and Disability After Acute Care and Critical Illness Hospitalizations in a Prospective Cohort of Older Adults. J Am Geriatr Soc. 2015; doi: 10.1111/jgs.13663

Ely EW, Wheeler AP, Thompson BT, Ancukiewicz M, Steinberg KP, Bernard GR. Recovery rate and prognosis in older persons who develop acute lung injury and the acute respiratory distress syndrome. Ann Intern Med. 2002; 136:25–36. [PubMed: 11777361]

Ewaschuk JB, Almasud A, Mazurak VC. Role of n-3 fatty acids in muscle loss and myosteatosis. Appl Physiol Nutr Metab. 2014; 39:654–62. DOI: 10.1139/apnm-2013-0423 [PubMed: 24869970]

Ferrante LE, Pisani MA, Murphy TE, Gahbauer EA, LeoSummers LS, Gill TM. Functional Trajectories Among Older Persons Before and After Critical Illness. JAMA Intern Med. 2015; 175:523–529. DOI: 10.1001/jamainternmed.2014.7889 [PubMed: 25665067]

Ferrante LE, Pisani MA, Murphy TE, Gahbauer EA, Leo-Summers LS, Gill TM. Factors Associated with Functional Recovery Among Older ICU Survivors. Am J Respir Crit Care Med. 2016; doi: 10.1164/rccm.201506-1256OC

Files DC, et al. A critical role for muscle ring finger-1 in acute lung injury-associated skeletal muscle wasting. Am J Respir Crit Care Med. 2012; 185:825–34. DOI: 10.1164/rccm.201106-1150OC [PubMed: 22312013]

Files DC, et al. Therapeutic exercise attenuates neutrophilic lung injury and skeletal muscle wasting. Sci Transl Med. 2015a; 7:278ra32.doi: 10.1126/scitranslmed.3010283

Files DC, Sanchez MA, Morris PE. A conceptual framework: the early and late phases of skeletal muscle dysfunction in the acute respiratory distress syndrome. Crit Care. 2015b; 19:266.doi: 10.1186/s13054-015-0979-5 [PubMed: 26134116]

Force ADT, et al. Acute respiratory distress syndrome: the Berlin Definition. JAMA. 2012; 307:2526–33. DOI: 10.1001/jama.2012.5669 [PubMed: 22797452]

Fukawa T, et al. Excessive fatty acid oxidation induces muscle atrophy in cancer cachexia. Nat Med. 2016; doi: 10.1038/nm.4093

Garvey SM, et al. Metabolomic profiling reveals severe skeletal muscle group-specific perturbations of metabolism in aged FBN rats. Biogerontology. 2014; 15:217–32. DOI: 10.1007/s10522-014-9492-5 [PubMed: 24652515]

Goodpaster BH, et al. The loss of skeletal muscle strength, mass, and quality in older adults: the health, aging and body composition study. J Gerontol A Biol Sci Med Sci. 2006; 61:1059–64. [PubMed: 17077199]

Hermans G, et al. Acute outcomes and 1-year mortality of intensive care unit-acquired weakness. A cohort study and propensity-matched analysis. Am J Respir Crit Care Med. 2014; 190:410–20. DOI: 10.1164/rccm.201312-2257OC [PubMed: 24825371]

Herridge MS, et al. Functional disability 5 years after acute respiratory distress syndrome. N Engl J Med. 2011; 364:1293–304. DOI: 10.1056/NEJMoa1011802 [PubMed: 21470008]

Jensen MV, et al. Compensatory responses to pyruvate carboxylase suppression in islet beta-cells. Preservation of glucose-stimulated insulin secretion. J Biol Chem. 2006; 281:22342–51. DOI: 10.1074/jbc.M604350200 [PubMed: 16740637]

Kamolrat T, Gray SR. The effect of eicosapentaenoic and docosahexaenoic acid on protein synthesis and breakdown in murine C2C12 myotubes. Biochem Biophys Res Commun. 2013; 432:593–8. DOI: 10.1016/j.bbrc.2013.02.041 [PubMed: 23438435]

Kumar KV, Rao SM, Gayani R, Mohan IK, Naidu MU. Oxidant stress and essential fatty acids in patients with risk and established ARDS. Clin Chim Acta. 2000; 298:111–20. [PubMed: 10876008]

Langen RC, et al. NF-kappaB activation is required for the transition of pulmonary inflammation to muscle atrophy. Am J Respir Cell Mol Biol. 2012; 47:288–97. DOI: 10.1165/rcmb.2011-0119OC [PubMed: 22538866]

Larsen AE, Crowe TC. Effects of conjugated linoleic acid on myogenic and inflammatory responses in a human primary muscle and tumor coculture model. Nutr Cancer. 2009; 61:687–95. DOI: 10.1080/01635580902898750 [PubMed: 19838943]

Li LO, et al. Compartmentalized acyl-CoA metabolism in skeletal muscle regulates systemic glucose homeostasis. Diabetes. 2015; 64:23–35. DOI: 10.2337/db13-1070 [PubMed: 25071025]

Manzano F, et al. Incidence of acute respiratory distress syndrome and its relation to age. J Crit Care. 2005; 20:274–80. DOI: 10.1016/j.jcrc.2005.05.008 [PubMed: 16253798]

Matthay MA, Ware LB, Zimmerman GA. The acute respiratory distress syndrome. J Clin Invest. 2012; 122:2731–40. DOI: 10.1172/JCI60331 [PubMed: 22850883]

Metter EJ, Lynch N, Conwit R, Lindle R, Tobin J, Hurley B. Muscle quality and age: cross-sectional and longitudinal comparisons. J Gerontol A Biol Sci Med Sci. 1999; 54:B207–18. [PubMed: 10362000]

Morley JE, Thomas DR, Wilson MMG. Cachexia: pathophysiology and clinical relevance. Am J Clin Nutr. 2006; 83:735–743. [PubMed: 16600922]

O'Connell TM, et al. Metabolomic analysis of cancer cachexia reveals distinct lipid and glucose alterations. Metabolomics. 2008; 4:216–225. DOI: 10.1007/s11306-008-0113-7

Pariza MW, Park Y, Cook ME. Conjugated linoleic acid and the control of cancer and obesity. Toxicol Sci. 1999; 52:107–10.

Picard M, et al. Mitochondrial dysfunction and lipid accumulation in the human diaphragm during mechanical ventilation. Am J Respir Crit Care Med. 2012; 186:1140–9. DOI: 10.1164/rccm.201206-0982OC [PubMed: 23024021]

Prabha PS, Das UN, Ramesh G, Kumar KV, Kamalakar V. Free radical generation, lipid peroxidation and essential fatty acids in patients with septicemia. Prostaglandins Leukot Essent Fatty Acids. 1991; 42:61–5. [PubMed: 2011612]

Prows DR, Gibbons WJ Jr, Smith JJ, Pilipenko V, Martin LJ. Age and Sex of Mice Markedly Affect Survival Times Associated with Hyperoxic Acute Lung Injury. PLoS One. 2015; 10:e0130936.doi: 10.1371/journal.pone.0130936 [PubMed: 26103466]

Pugh TD, et al. A shift in energy metabolism anticipates the onset of sarcopenia in rhesus monkeys. Aging Cell. 2013; 12:672–81. DOI: 10.1111/acel.12091 [PubMed: 23607901]

Quinlan GJ, Lamb NJ, Evans TW, Gutteridge JM. Plasma fatty acid changes and increased lipid peroxidation in patients with adult respiratory distress syndrome. Crit Care Med. 1996; 24:241–6. [PubMed: 8605795]

Rodriguez JE, et al. The ubiquitin ligase MuRF1 regulates PPARalpha activity in the heart by enhancing nuclear export via monoubiquitination. Mol Cell Endocrinol. 2015; 413:36–48. DOI: 10.1016/j.mce.2015.06.008 [PubMed: 26116825]

Rubenfeld GD, et al. Incidence and outcomes of acute lung injury. N Engl J Med. 2005; 353:1685–93. DOI: 10.1056/NEJMoa050333 [PubMed: 16236739]

Smith HJ, Lorite MJ, Tisdale MJ. Effect of a cancer cachectic factor on protein synthesis/degradation in murine C2C12 myoblasts: modulation by eicosapentaenoic acid. Cancer Res. 1999; 59:5507–13. [PubMed: 10554027]

Tarnopolsky MA, Safdar A. The potential benefits of creatine and conjugated linoleic acid as adjuncts to resistance training in older adults. Appl Physiol Nutr Metab. 2008; 33:213–27. DOI: 10.1139/H07-142 [PubMed: 18347674]

Tian M, Kliewer KL, Asp ML, Stout MB, Belury MA. c9t11-Conjugated linoleic acid-rich oil fails to attenuate wasting in colon-26 tumor-induced late-stage cancer cachexia in male CD2F1 mice. Mol Nutr Food Res. 2011; 55:268–77. DOI: 10.1002/mnfr.201000176 [PubMed: 20827675]

Wu JY, et al. ENU mutagenesis identifies mice with mitochondrial branched-chain aminotransferase deficiency resembling human maple syrup urine disease. J Clin Invest. 2004; 113:434–40. DOI: 10.1172/JCI19574 [PubMed: 14755340]

Xia J, Psychogios N, Young N, Wishart DS. MetaboAnalyst: a web server for metabolomic data analysis and interpretation. Nucleic Acids Res. 2009; 37:W652–60. DOI: 10.1093/nar/gkp356 [PubMed: 19429898]

Xia J, Sinelnikov IV, Han B, Wishart DS. MetaboAnalyst 3.0—making metabolomics more meaningful. Nucleic Acids Res. 2015; 43:W251–7. DOI: 10.1093/nar/gkv380 [PubMed: 25897128]

Xia J, Sinelnikov IV, Wishart DS. MetATT: a web-based metabolomics tool for analyzing time-series and two-factor datasets. Bioinformatics. 2011; 27:2455–6. DOI: 10.1093/bioinformatics/btr392 [PubMed: 21712247]

Zulet MA, Marti A, Parra MD, Martinez JA. Inflammation and conjugated linoleic acid: mechanisms of action and implications for human health. J Physiol Biochem. 2005; 61:483–94. [PubMed: 16440602]

Non-standard abbreviations

ALI acute lung injury

ARDS	acute respiratory distress syndrome
LPS	lipopolysaccharide
GAS	gastrocnemius
EDL	extensor digitorum longus
SOL	soleus
TA	tibialis anterior

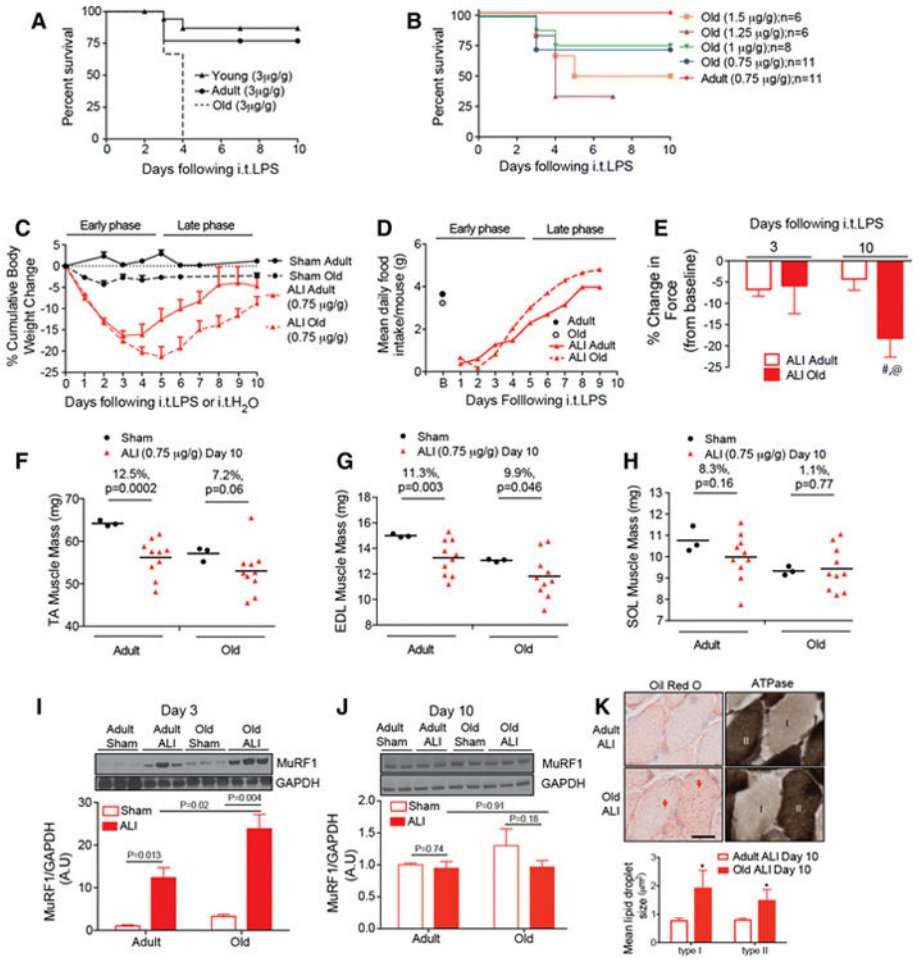

Figure 1. Lung injury in old mice results in increased mortality and prolonged muscle weakness

A) Survival curves for young (2 month old), adult (6-month old) and old (20-month old) acute lung injury (ALI) mice following high dose (3μg/g) LPS. N=37/very young, N=13/adult, N=3/old. **B)** LPS dose titration in old ALI mice, at doses ranging from 0.75 to 1.5 μg/g. N=11/adult (0.75μg/g), N=11/old (0.75 μg/g), N=8/old (1μg/g). N=6/old (1.25 μg/g). N=6/old (1.5 μg/g) **C)** Cumulative body weight changes in adult and old Sham and ALI (0.75 μg/g) mice following intratracheal (i.t.) H_2O or i.t. LPS. N=3 for Sham groups, N=10 ALI groups. **D)** Mean daily food intake in Adult and Old baseline and ALI mice. N=6 per group. **E**) The percent change in maximal tetanic force by ankle plantarflexion generated at 125 Hz stimulation at days 3 and 10 following 0.75 μg/g or 1 μg/g LPS was compared to baseline values in individual animals; #Old baseline vs Old Day 10 p=0.007, @Adult ALI Day 10 vs Old ALI Day 10 p=0.004, N=10 Adult baseline, N=13 Old baseline, N=6 ALI Adult day 3, N=6 ALI Old day 3, N=10 ALI Adult day 10, N=7 ALI Old day 10. Sham or ALI (0.75 μg/g) muscle wet weights of the **F)** tibialis anterior (TA) **G)** extensor digitorum longus (EDL) or **H)** soleus (SOL) muscles at day 10. Gastrocnemius protein lysates from **I)** Day 3 and **J)** Day 10 ALI (0.75 μg/g) or Sham mice were probed for MuRF1 expression, normalized GAPDH and quantified by densitometry (N=3 for Sham mice, N=5-6 for ALI groups). **K)** Staining for intramyocellular lipid (IMCL) accumulation (red arrows) in type I

and type II myofibers of the soleus in Adult and Old ALI mice at day 10. N=3/group, *p=0.04 for group differences.

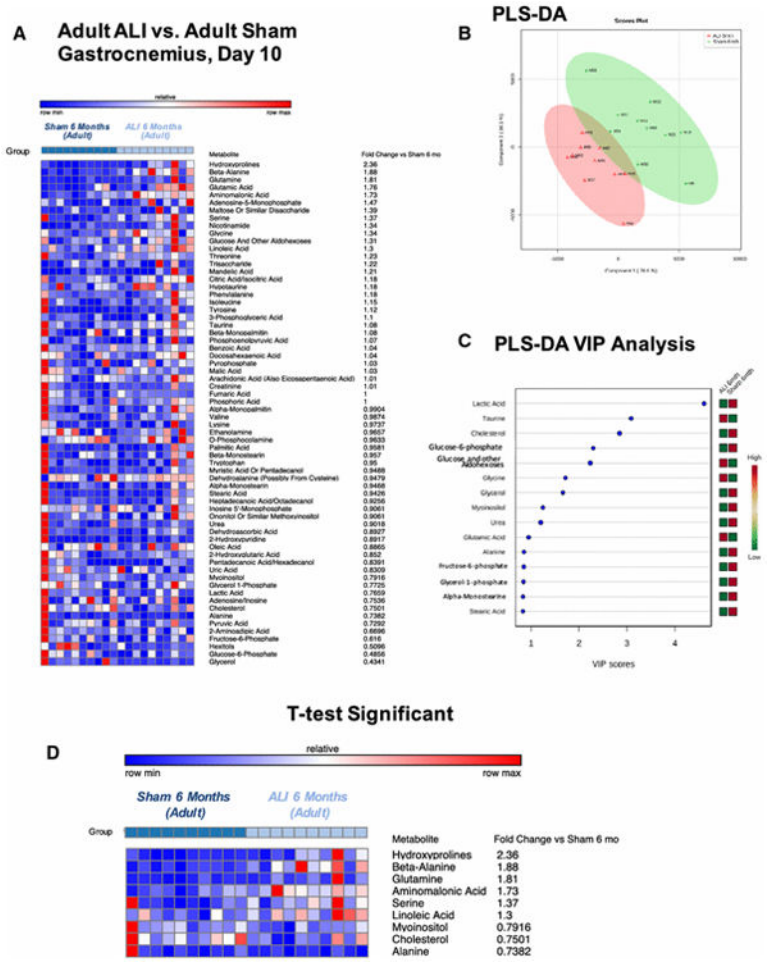

Figure 2. Non-targeted metabolomics of adult ALI muscle at day 10 compared to adult Sham mice

A) Heat map of metabolites identified by non-targeted GC/MS analysis. **B)** Partial least squares-discriminant analysis (PLS-DA). **C)** Partial least squares-discriminant analysis (PLS-DA) and variable importance in the projection (VIP) analysis and **D)** Heat map of t test significant ($p<0.05$) results. N=10/group.

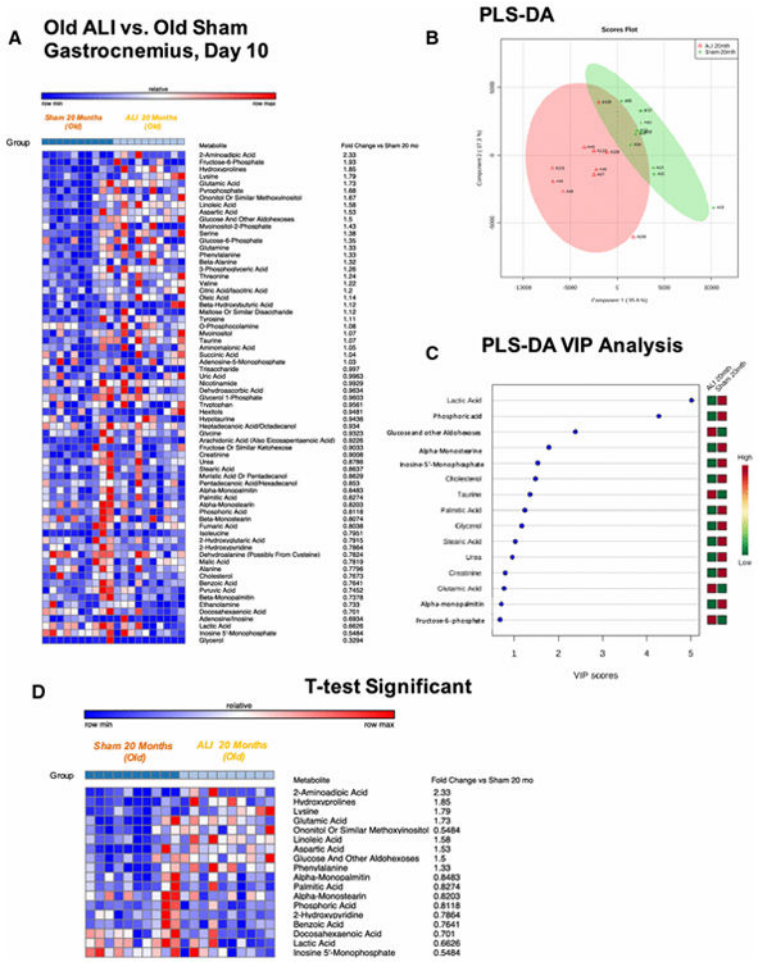

Figure 3. Non-targeted metabolomics of old ALI muscle at day 10 compared to old Sham mice

A) Heat map of metabolites identified by non-targeted GC/MS analysis. **B)** Partial least squares-discriminant analysis (PLS-DA) **C)** Partial least squares-discriminant analysis (PLS-DA) and variable importance in the projection (VIP) analysis and **D)** Heat map of t test significant ($p<0.05$) results. N=10/group.

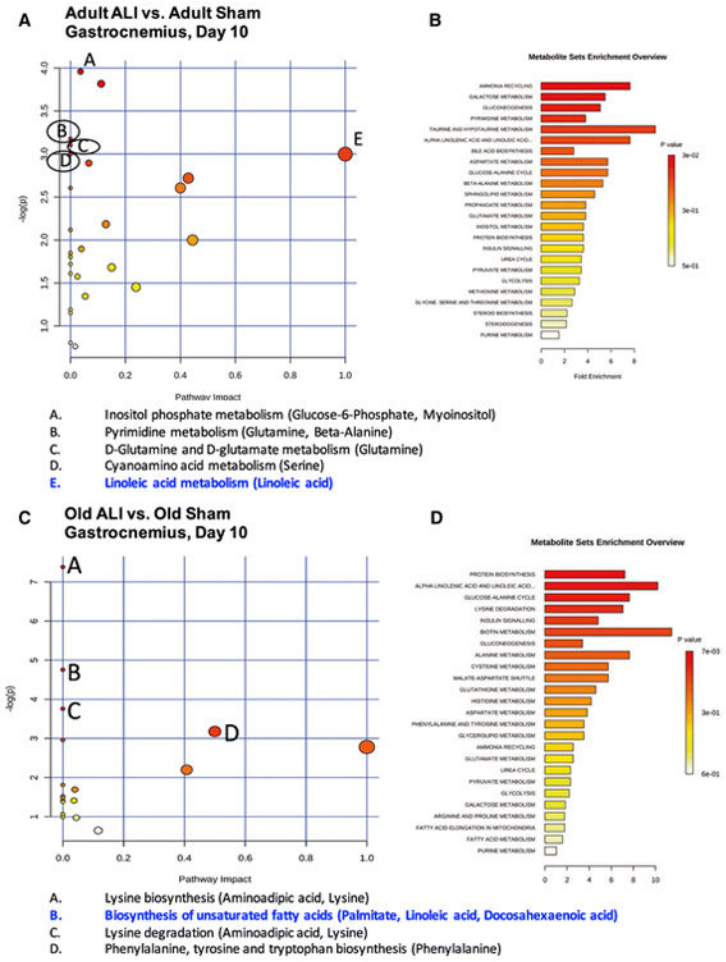

Figure 4. Pathway enrichment of significant metabolites found in adult ALI muscle compared to adult Sham mice

A) Pathway enrichment analysis for adult (6-month) acute lung injury compared to Sham controls. *a-e* indicates top pathways identified, along with the specific significant metabolites found that placed it in this category. **B)** Enrichment by metabolite sets determined from VIP and t-test significant metabolites identified in adult ALI mice compared to their adult Sham. **C)** Pathway enrichment analysis for old ALI compared to old Sham *a-e* indicates top pathways identified, along with the specific significant metabolites found that placed it in this category. **D)** Enrichment by metabolite sets determined from VIP and t-test significant metabolites identified in old ALI compared to old Sham. a-e indicates top pathways identified, along with the specific significant metabolites found that placed it in this category.

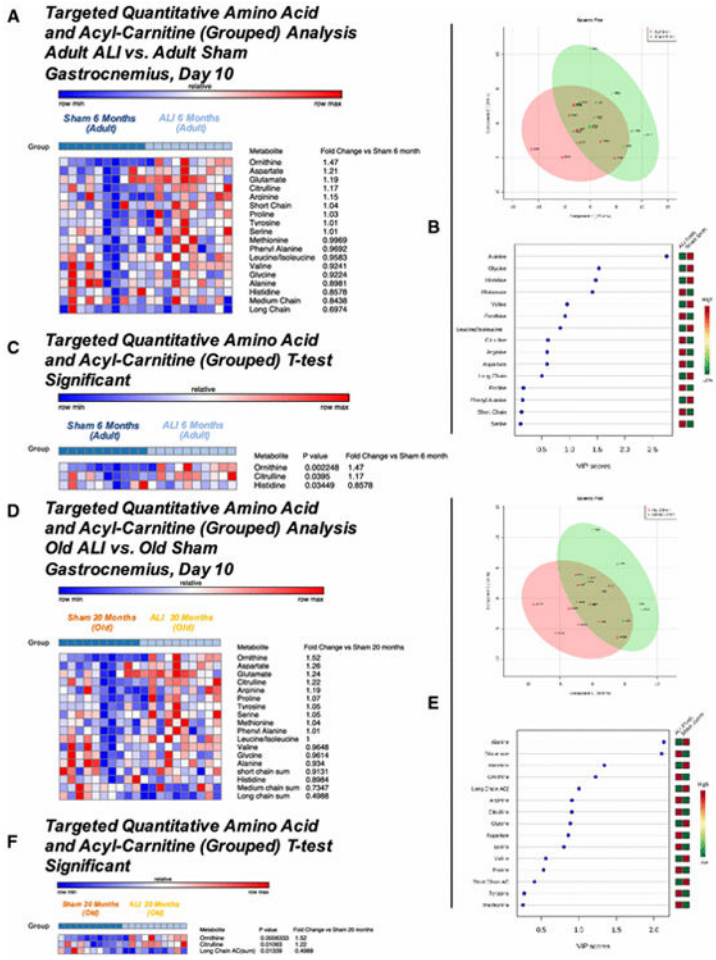

Figure 5. Quantitative targeted metabolomics analysis of grouped acyl carnitines and amino acids in adult and old ALI and Sham mice

Targeted metabolomic analysis of adult ALI muscle showing **A)** Heat map of grouped acyl carnitines and amino acids, **B)** Partial least squares-discriminant analysis (PLS-DA) with variable importance in the projection (VIP) analysis, and **C)** Heat map of t test significant results. Targeted metabolomic analysis of old ALI showing **D)** Heat map of grouped acyl carnitines and amino acids, **E)** Partial least squares-discriminant analysis (PLS-DA) with variable importance in the projection (VIP) analysis, and **F)** Heat map of t test significant ($p<0.05$) results. N=10/group.

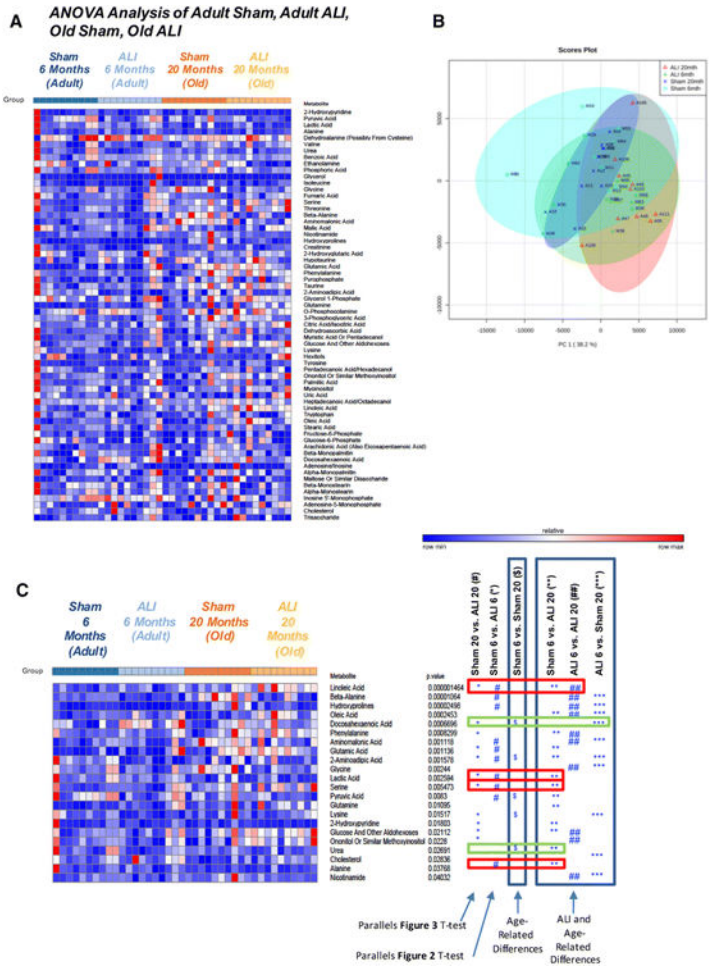

Figure 6. ANOVA analysis of non-targeted metabolomics from both adult and old ALI and Sham muscle

A) Heat map and **B)** Principal components analysis of metabolites identified by non-targeted GC/MS analysis among all groups of comparison. **C)** Summary heat map of OneWay ANOVA significant metabolites, determined by Fisher-LSD post hoc test results. Metabolites identified to be altered by post hoc test, and classified depending on the factor that induced the changes. Six Fisher LSD post hoc comparisons were made: *, Sham 20 vs. ALI 20 (Column 1); #, Sham 6 vs. ALI 6 (Column 2); $, Sham 6 vs. Sham 20 (Column 3); **, Sham 6 vs. ALI 20 (Column 4); ##, ALI 6 vs. ALI 20 (Column 5); ***, ALI 6 vs. Sham 20 (Column 6). Metabolites previously related to ALI and age are boxed in red; metabolites related to age only are shown in green. Significance defined as $p<0.05$.

22 metabolites were significantly different using ANOVA analysis (Figure 6C). Further inter-group analysis identified age-dependent differences, between old Sham and adult Sham muscle in metabolites including docosahexaenoic acid, 2-aminoadipic acid, pyruvic acid, lysine, and ononitol (see $, Figure 6C). In addition to these metabolites that were different between the adult Sham and old Sham muscle, we also evaluated metabolite alterations in both old groups (old Sham and old ALI) and identified urea and docosahexanoic acid (DHA) (Supplemental Figure 3A). To identify metabolites that were significantly altered in ALI regardless of age, we identified altered metabolites found in both ALI groups

(SupplementalFigure 3A). DHA was significantly increased in an age-dependent fashion (Supplemental Figure 3B), whereas linoleic acid was significantly increased in with ALI conditions regardless of age (Supplemental Figure 3C). In addition, lactate, serine, and alanine were differentially regulated in ALI conditions regardless of age (Supplemental Figure 3A).